High pressure nano-imaging

Wenge Yang

HPSynC, Geophysical Laboratory, Carnegie Institution of Washington

GL Efree highlight
Jan. 28, 2015

ARGONNE NATIONAL LABORATORY

CARNEGIE INSTITUTION OF WASHINGTON · 1902 ·

Bone X-ray (radiography)

An x-ray radiograph is a noninvasive medical test that helps physicians diagnose and treat medical conditions. Imaging with x-rays involves exposing a part of the body to a small dose of ionizing radiation to *produce pictures of the inside of the body*. X-rays are the oldest and most frequently used form of medical imaging.

(RadiologyInfo.org)

三维CT成像

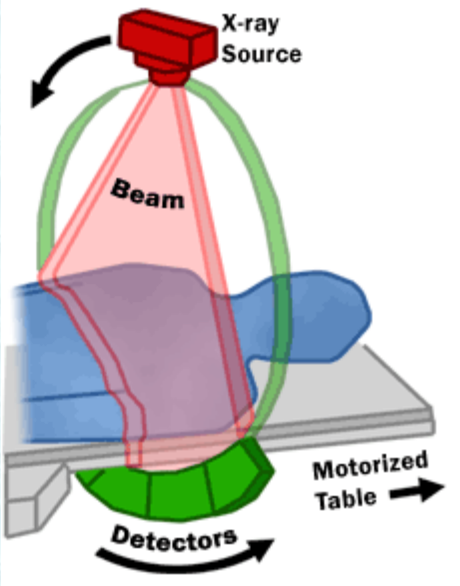

An example of a single-slice CT image of the brain.

Description
Computed tomography (CT) scanning, also called computerized axial tomography (CAT) scanning, is a medical imaging procedure that uses x-rays to show cross-sectional images of the body.
A CT imaging system produces cross-sectional images or "slices" of areas of the body, like the slices in a loaf of bread. These cross-sectional images are used for a variety of diagnostic and therapeutic purposes.

Uses
CT can help diagnose or rule out a disease or condition. CT has become recognized as a valuable medical tool, for:
Diagnosis of disease, trauma, or abnormality;
Planning, guiding, and monitoring therapy.

Hard x-ray imaging methods

Nondestructive, phase contrast, scanning probe, diffraction contrast, tomography, topography ……

Basically there are two experimental approaches:

Full field imaging， scanning probe

In both cases, there must be a *physical property to give contrast*.
They could be magnetic domain, electric domain, phase, orientation, density, chemical composition, strain, etc.

Soft X-ray Imaging

Mostly used for biologic materials, soft matter, nanomagnetism

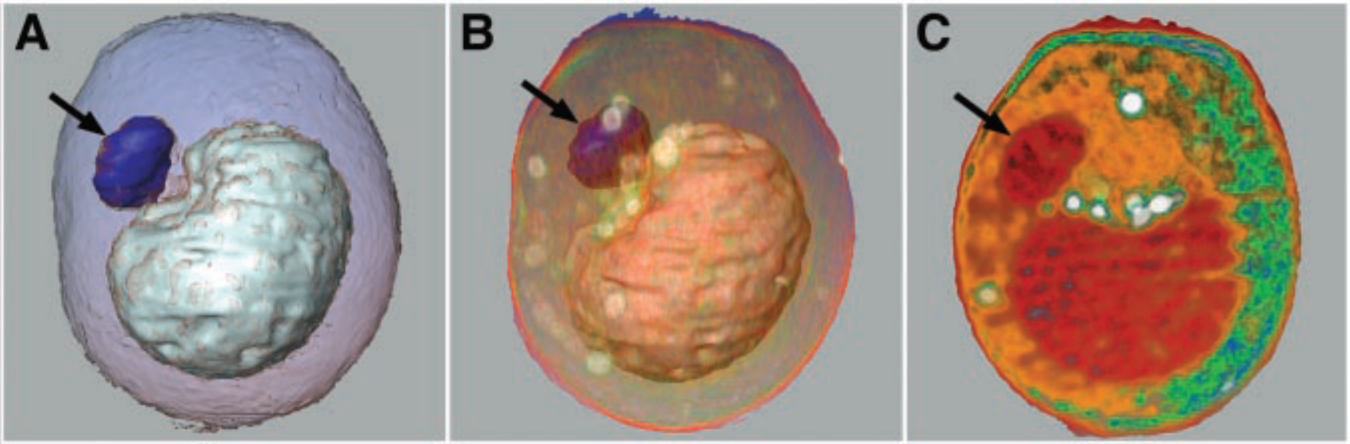

Cryo X-ray tomography of whole yeast, *S. cerevisiae, viewed using several processing* algorithms after reconstruction.

C.A. Larabell and M.A LeGros, **X-ray Tomography Generates 3-D Reconstructions of the Yeast, *Saccharomyces cerevisiae, at 60-nm* Resolution**
Molecular Bio. Cell 15, 957 (04)

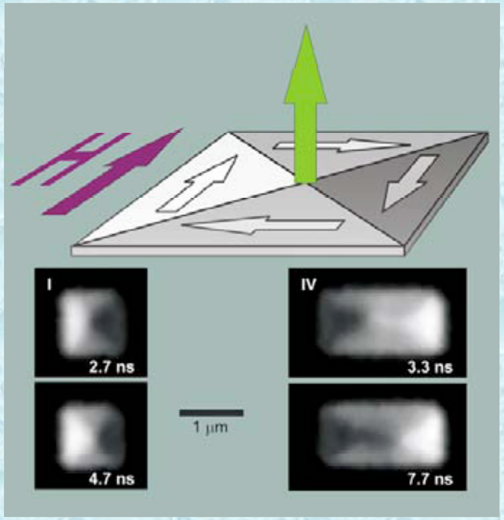

Vortex core – driven magnetization dynamics

Time-resolved x-ray imaging shows that the magnetization dynamics of a micron-sized pattern containing a ferromagnetic vortex is determined by its chirality

Time-resolved x-ray Photoemission electron microscope (PEEM)
Was used to resolve the motion of magnetic vortices of micro-pattern in response to an excitation field pulse.

Choe et al. Science 304, 420 (2004)

Some applications of 3d imaging

- Coherent diffraction imaging on the internal strain and morphology of nanocrystals

- Charge disproportion mapping during pressure induced phase transition

- Direct measurement of volume vs. Pressure - EoS of amorphous materials

- High pressure imaging outlook

Bragg CDI

Coherent diffraction imaging on nanoscale morphology and strain mapping

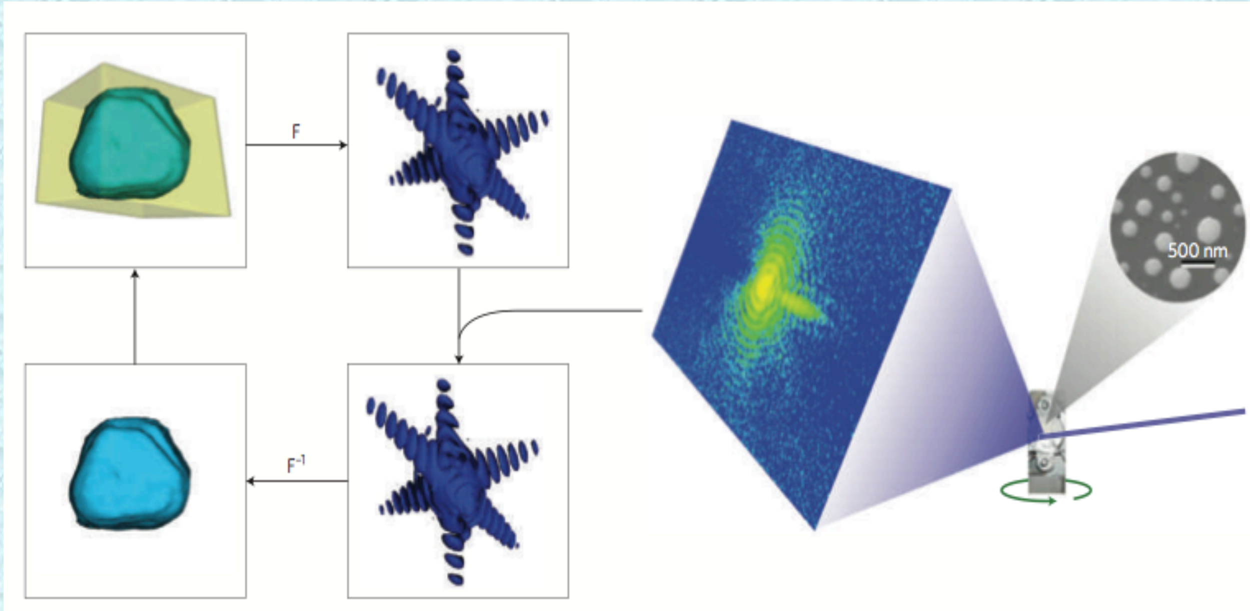

Phase retrieval algorithm

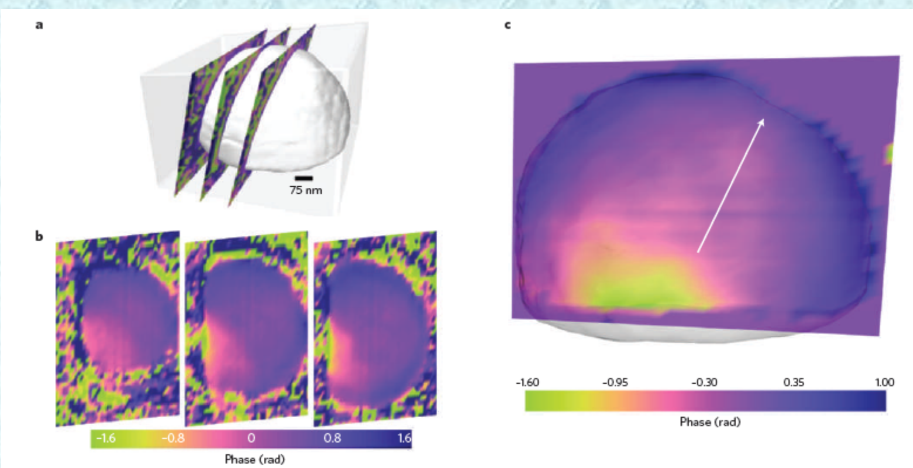

Figure 3 | Visualization of strain inside a Pb nanocrystal. a, Schematic showing cut-planes passing through an isosurface of the density of the Pb nanocrystal studied with CXD. **b**, The phase (in radians) is shown as colours on the extracted planes. **c**, The phase on one section of the same crystal plane after correction for refraction effects[42]. The contact strain due to the substrate is negative (green) whereas the surface strain is positive (blue). The surface strain is diminished on the (111) facet itself[42]. Parts **a** and **b** reprinted with permission from ref. 40. © 2006 NPG; part **c** reprinted with permission from ref. 42. © 2007 APS.

nature materials | INSIGHT | REVIEW ARTICLES
PUBLISHED ONLINE: 24 MARCH 2009 | DOI: 10.1038/NMAT2400

Coherent X-ray diffraction imaging of strain at the nanoscale

Ian Robinson[1*] and Ross Harder[2]

Bragg CDI principle

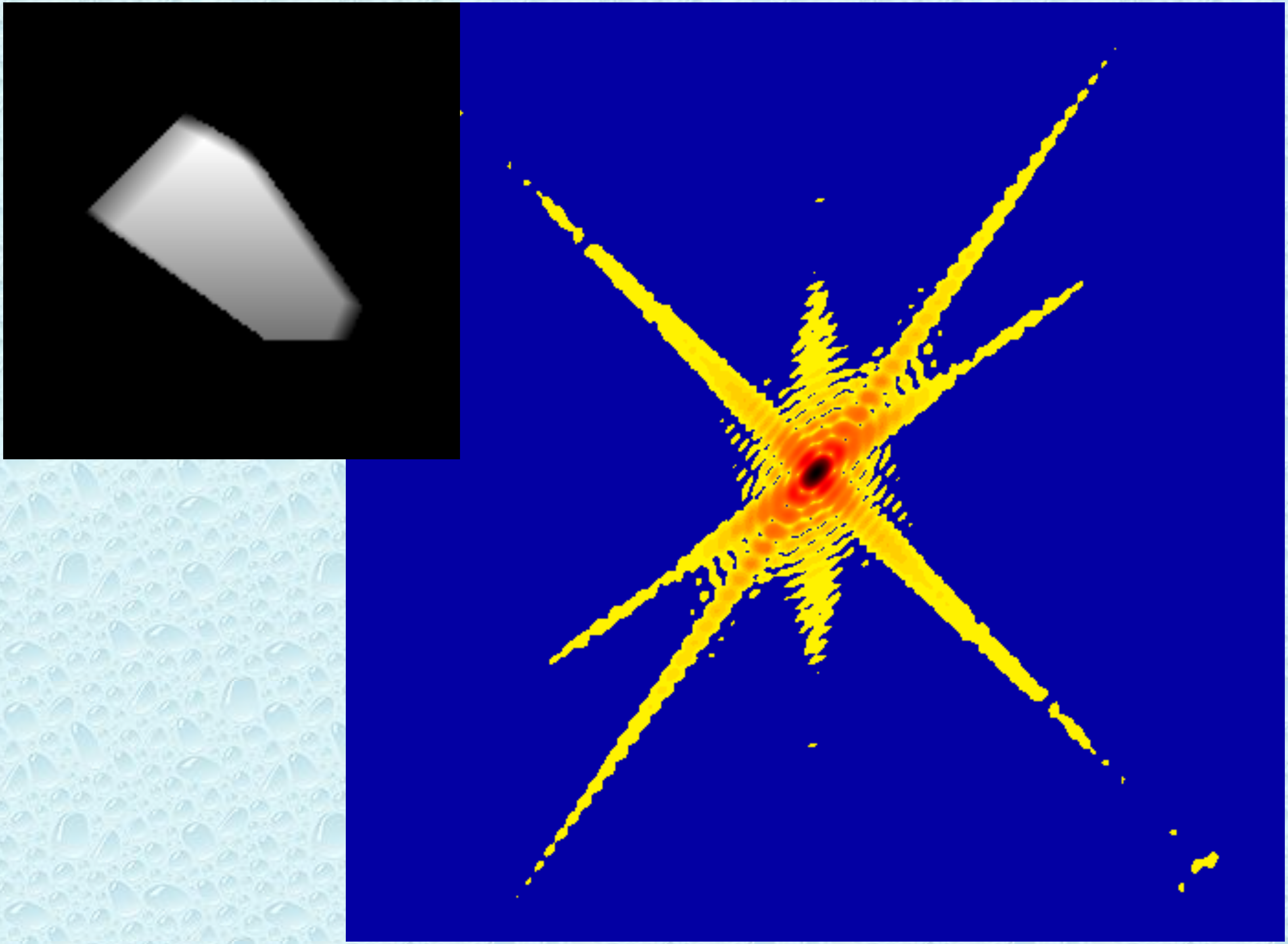

Coherent diffraction imaging (CDI) on single crystal under high pressure

Experimental setup at 34ID-C, APS

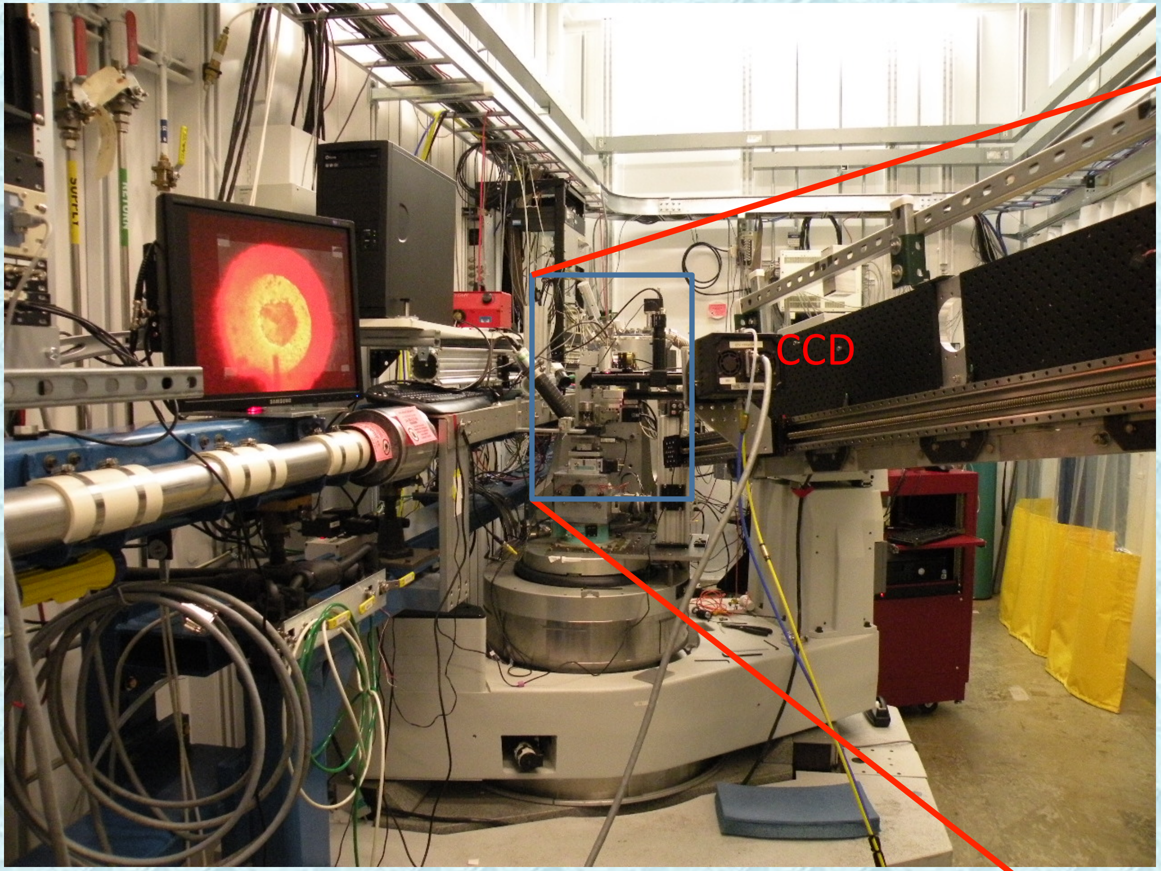

Panoramic DAC on a kinematical mount

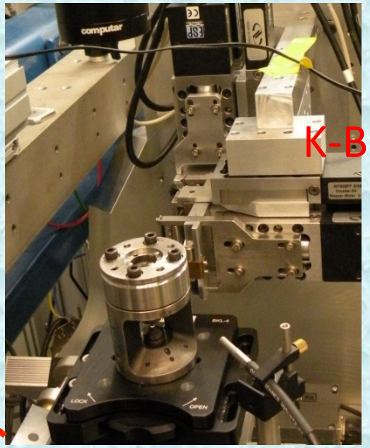

Bragg CDI for 3D strain map

Sample and experimental schematic

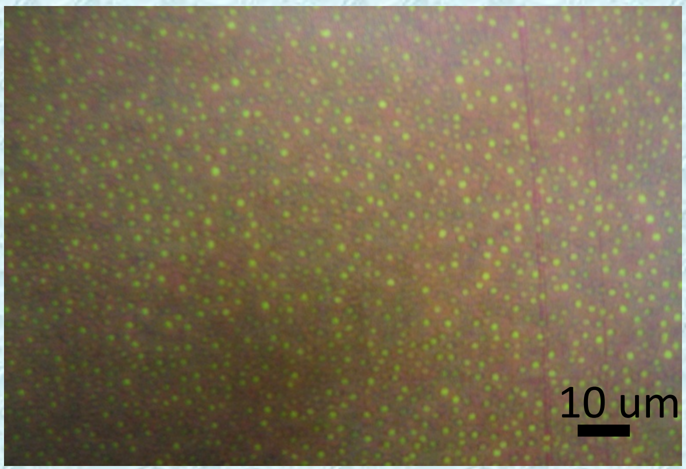

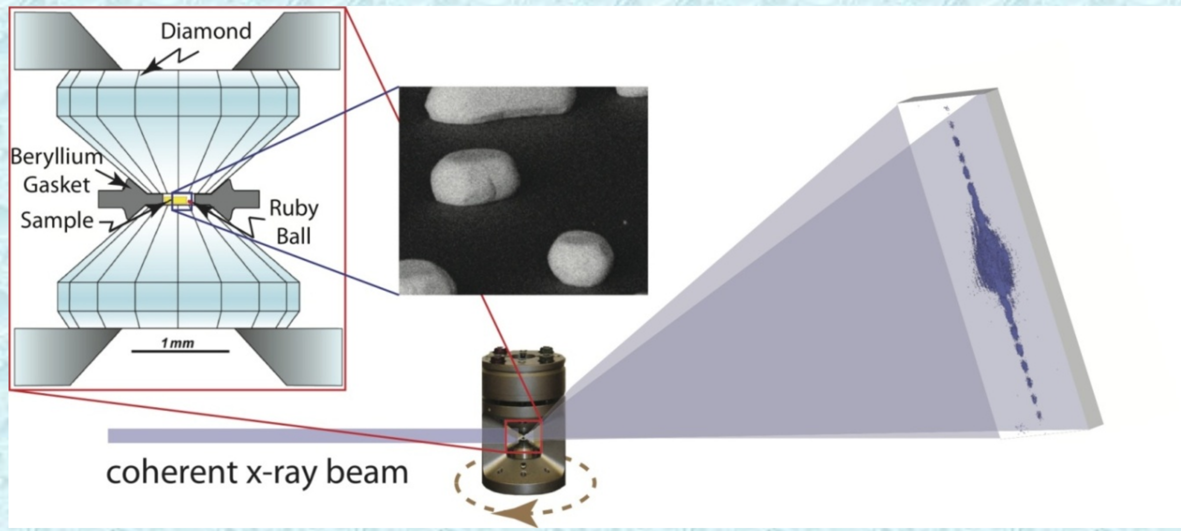

Average 300 nm size Au single crystals grown on Si wafer

Yang et al, nature Comm. (2013)

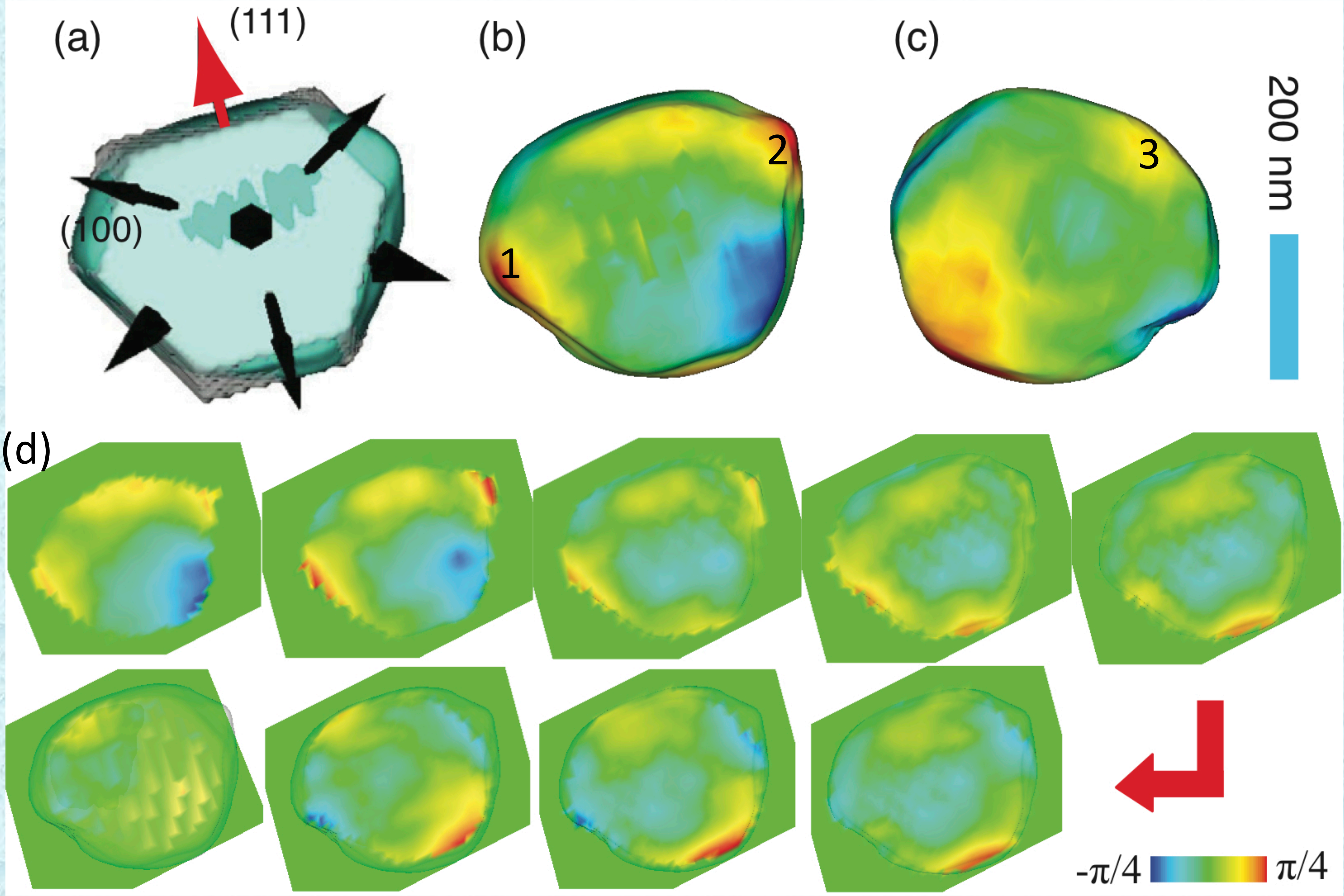

3d morphology and strain distribution at pressure 1.7 GPa

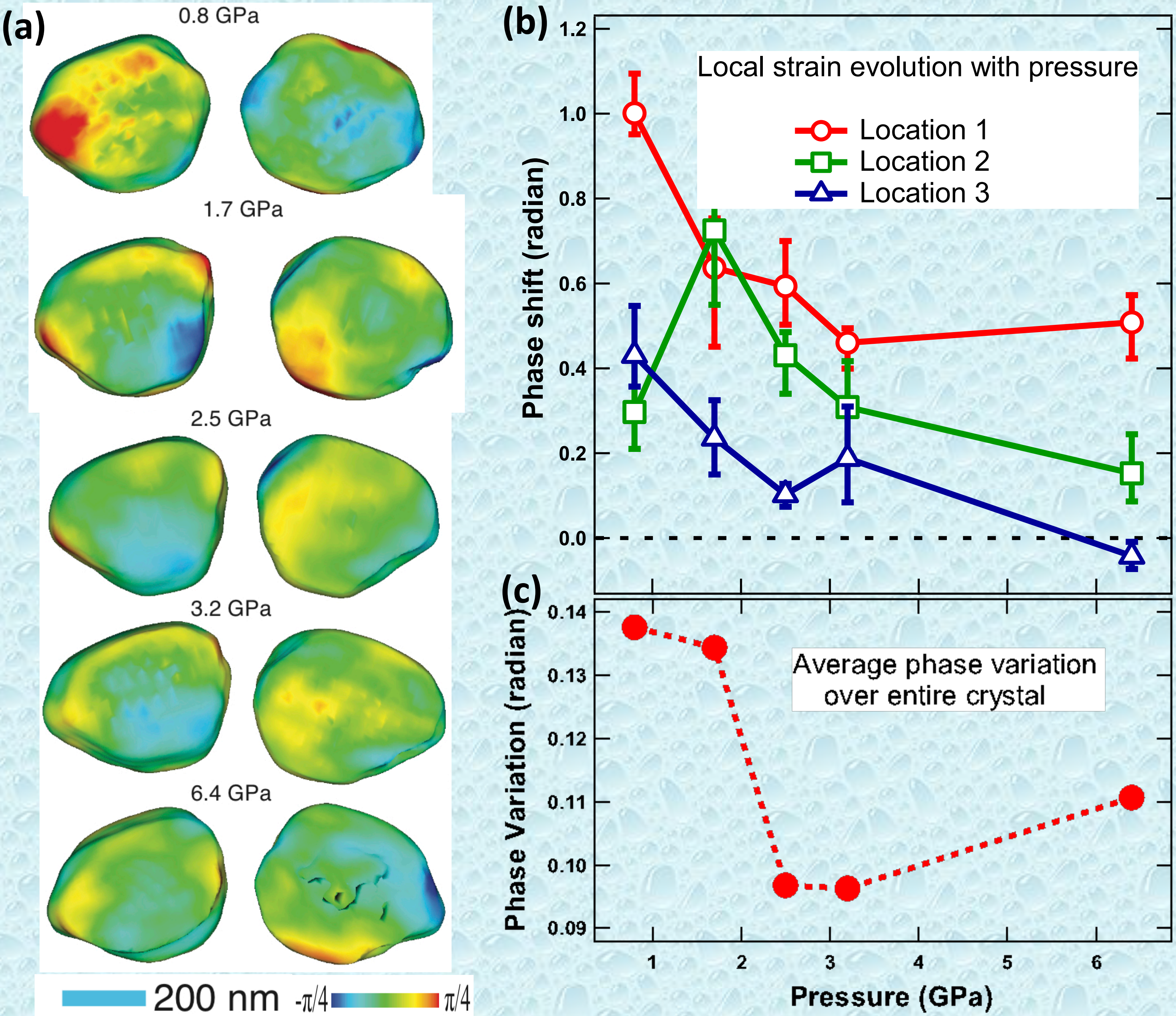

Phase evolution vs. applied pressure

Small angle CDI for 3D density map

Coherent X-ray diffraction Microscopy for nanoscience and biology (small angle geometry)

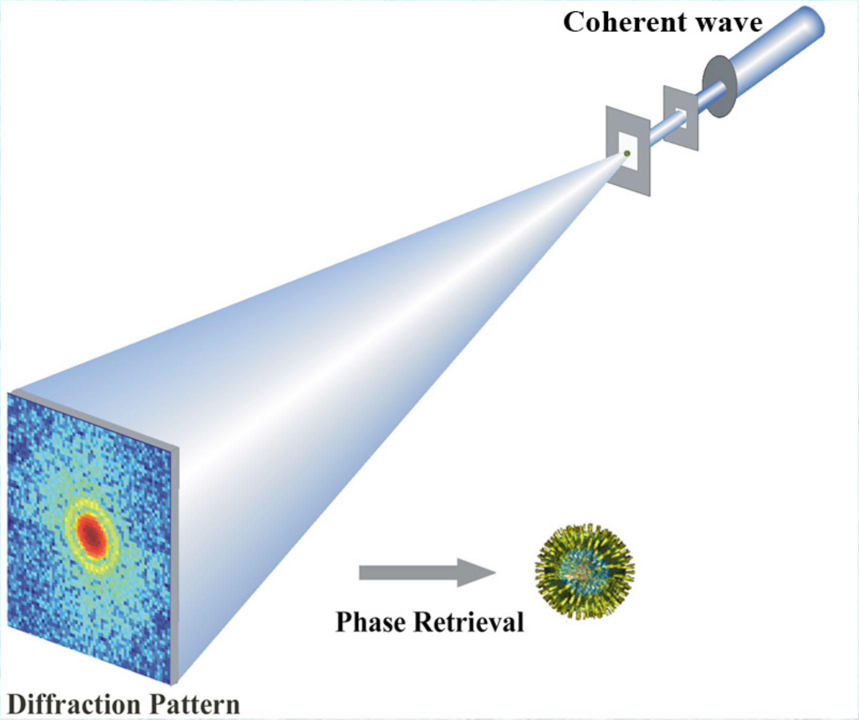

Schematic layout of coherent diffraction microscopy. The oversampled diffraction intensities are measured from a finite specimens, and then directly phased to obtain a high resolution image.

Limitation: missing data at the center of diffraction pattern
Advantage: single-shot imaging for 3d (could be used in x-ray free electron lasers), non-crystalline specimens

From John Miao, UCLA

Sample studied: San Carlos + 10wt% Fe-S, 6 GPa + 1800 C for 1 hour

Single CDI 2d reconstruction STXM

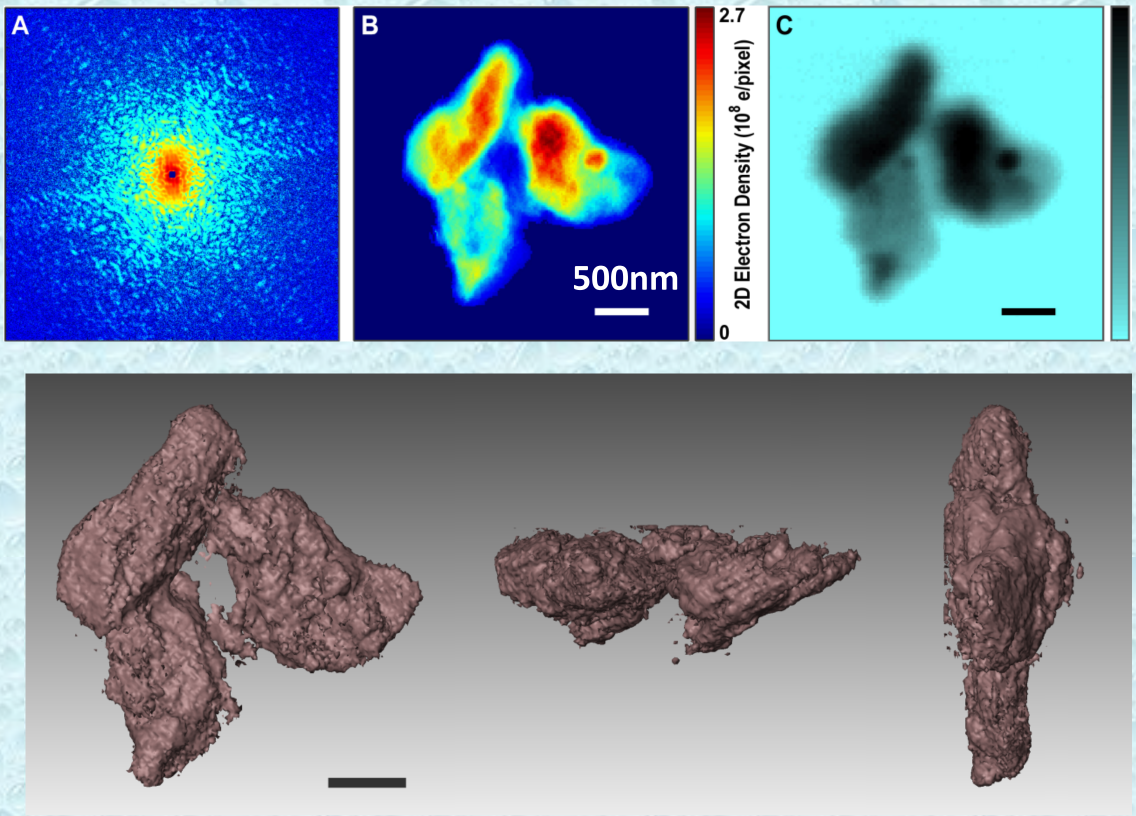

3d reconstruction from 27 2d diffraction patterns covering -69.4˚ to 69.4˚

Absolute electron density map

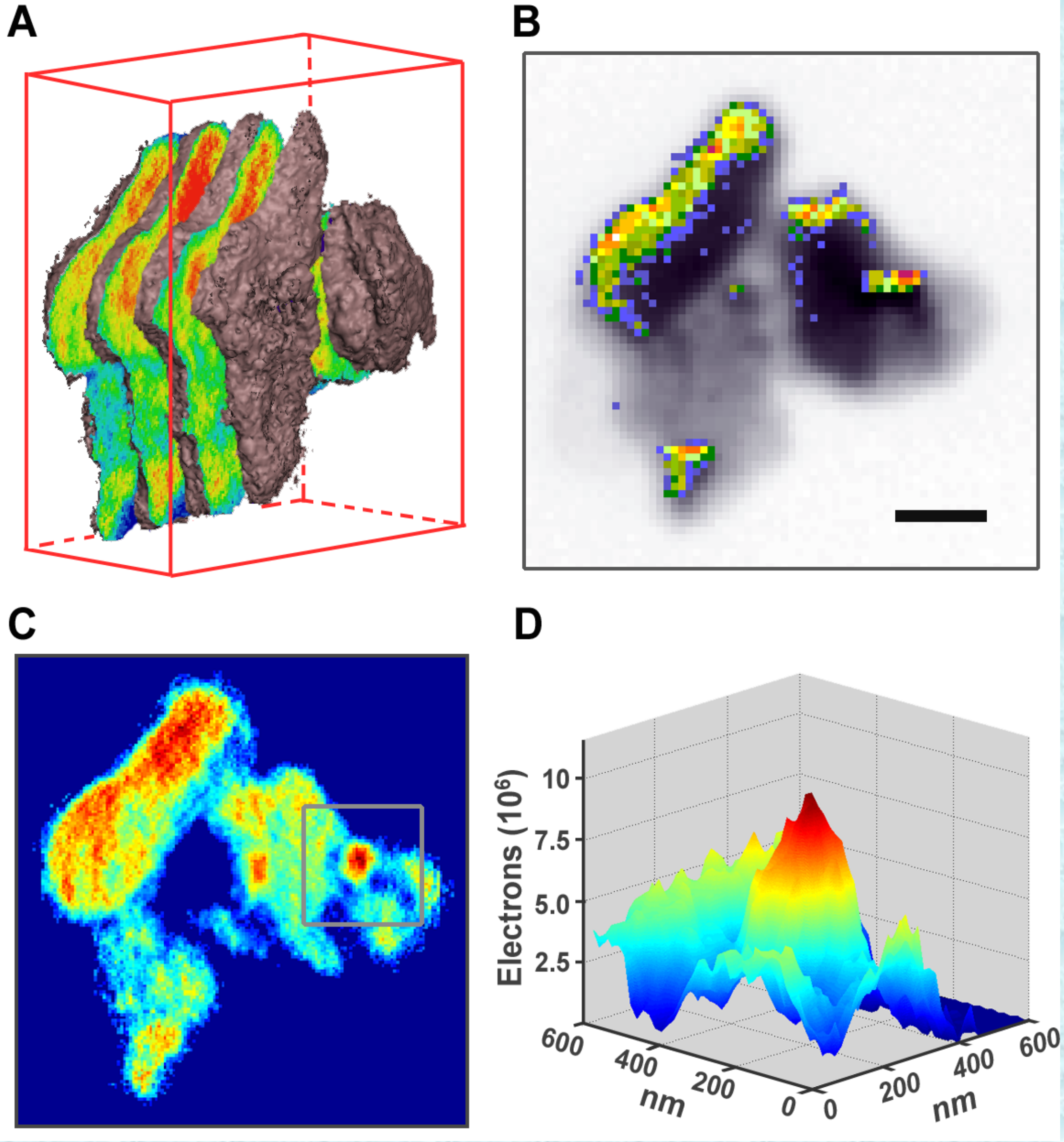

3d mass density

3d nanoscale mass density

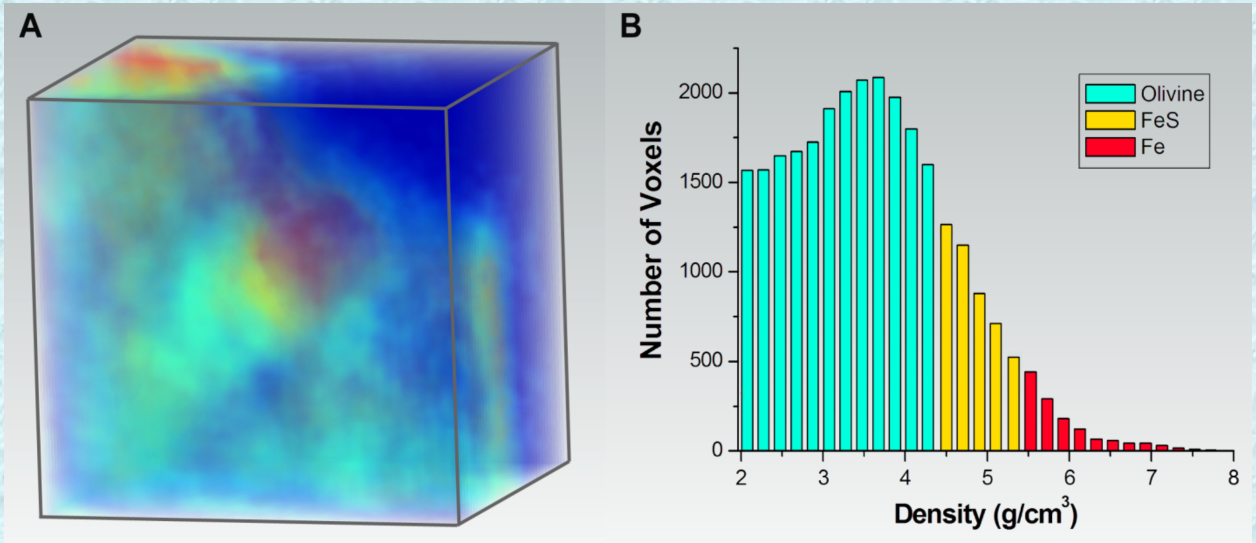

H. Jiang et al. PRL, 2013

3d tomography on the shock-recovered samples

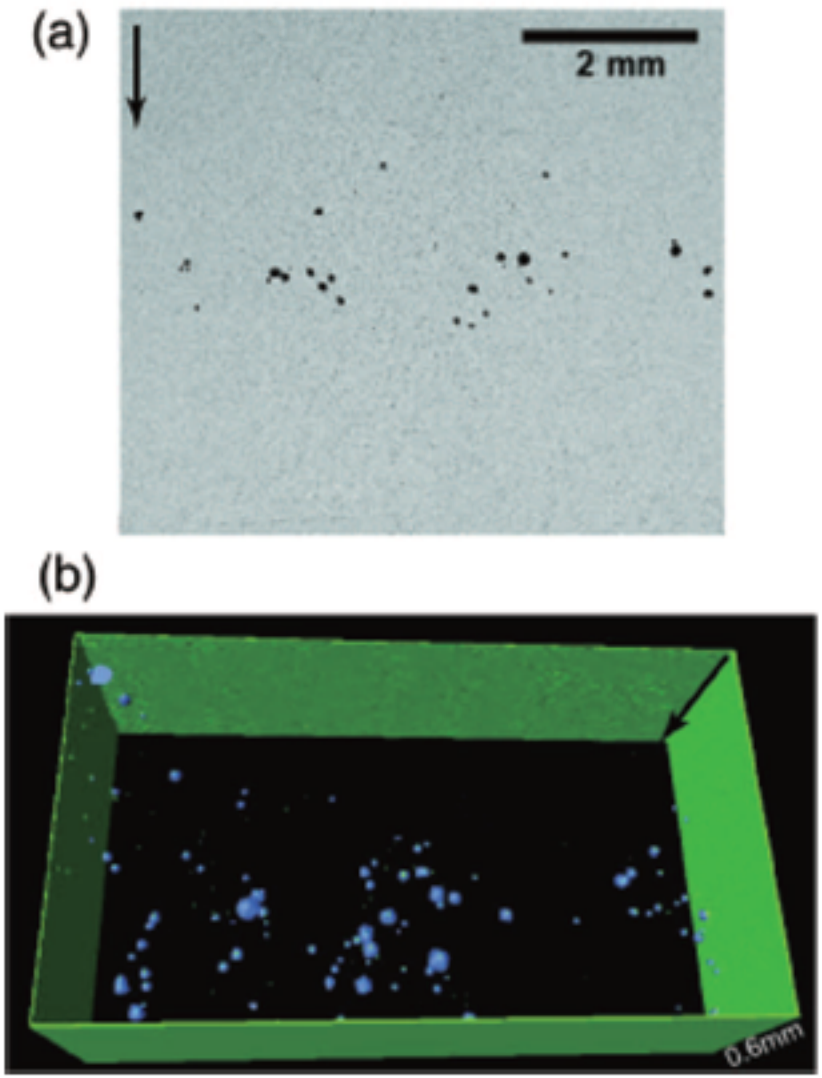

FIG. 1. 2D and 3D void distributions in shock-recovered pure Al sample Al010b (u_{flyer} = 149.6 m/s): (a) An optical micrograph of a cross-section. (b) A 0.6 mm thick slice from x-ray tomography, cut perpendicular to the shock direction. The arrows indicate shock direction. The box dimensions in (b) are 0.6 mm ×2 mm × 2 mm.

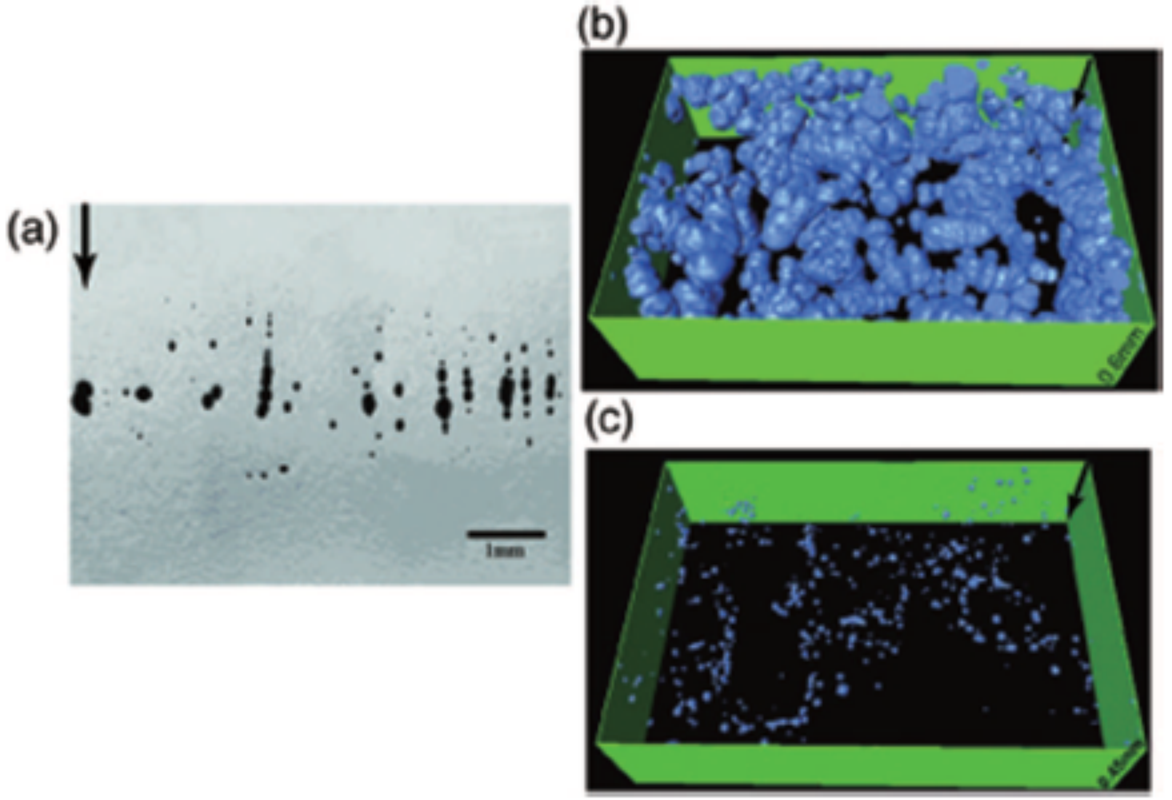

FIG. 2. 2D and 3D void distributions in shock-recovered pure Al sample Al006b (u_{flyer} = 196.9 m/s): (a) An optical micrograph of a cross-section. (b) A 0.6 mm thick slice near the spall plane and (c) a 0.45 mm thick slice far from the spall plane, cut perpendicular to the shock direction. The box dimensions in (b) and (c) are 0.6 mm × 2 mm × 2 mm and 0.45 mm × 2 mm × 2 mm, respectively. The arrows indicate shock direction.

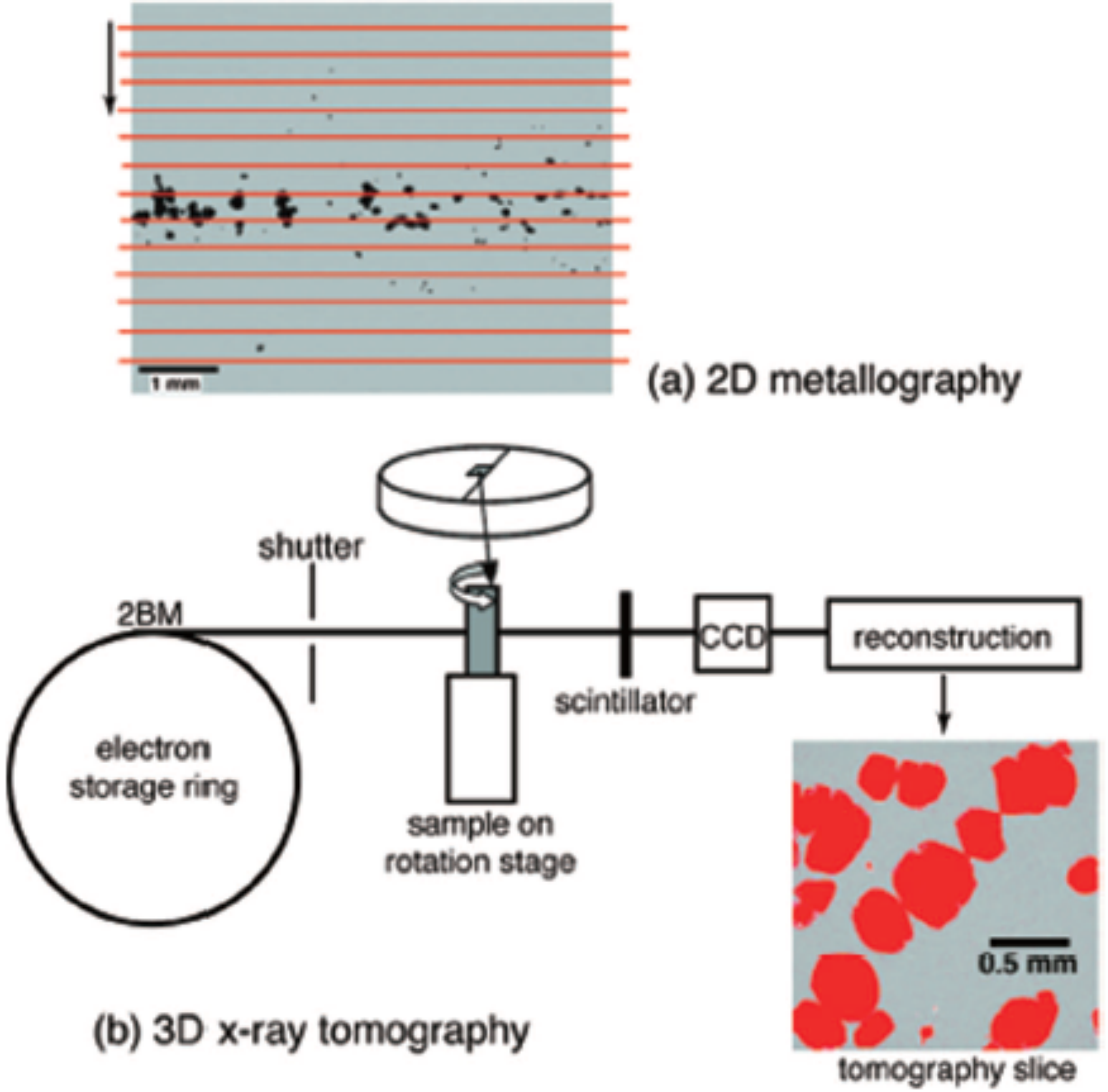

FIG. 3. (a) Illustration of 2D metallography for measuring damage profiles (the micrograph is for Al022b). (b) Schematic for 3D x-ray tomography at the APS (Advanced Photon Source) beamline 2BM. CCD: charge coupled device. The arrow in (a) indicates shock direction.

Meilan Qi et al. A metallographt and x-ray tomography study of spall damage in ultrapure Al, ACS Advances, 4, 077118 (2014)

3D TXM Nano-tomography

Transmission x-ray microscopy (TXM) setup at APS-32IDC and SSRL-6.2

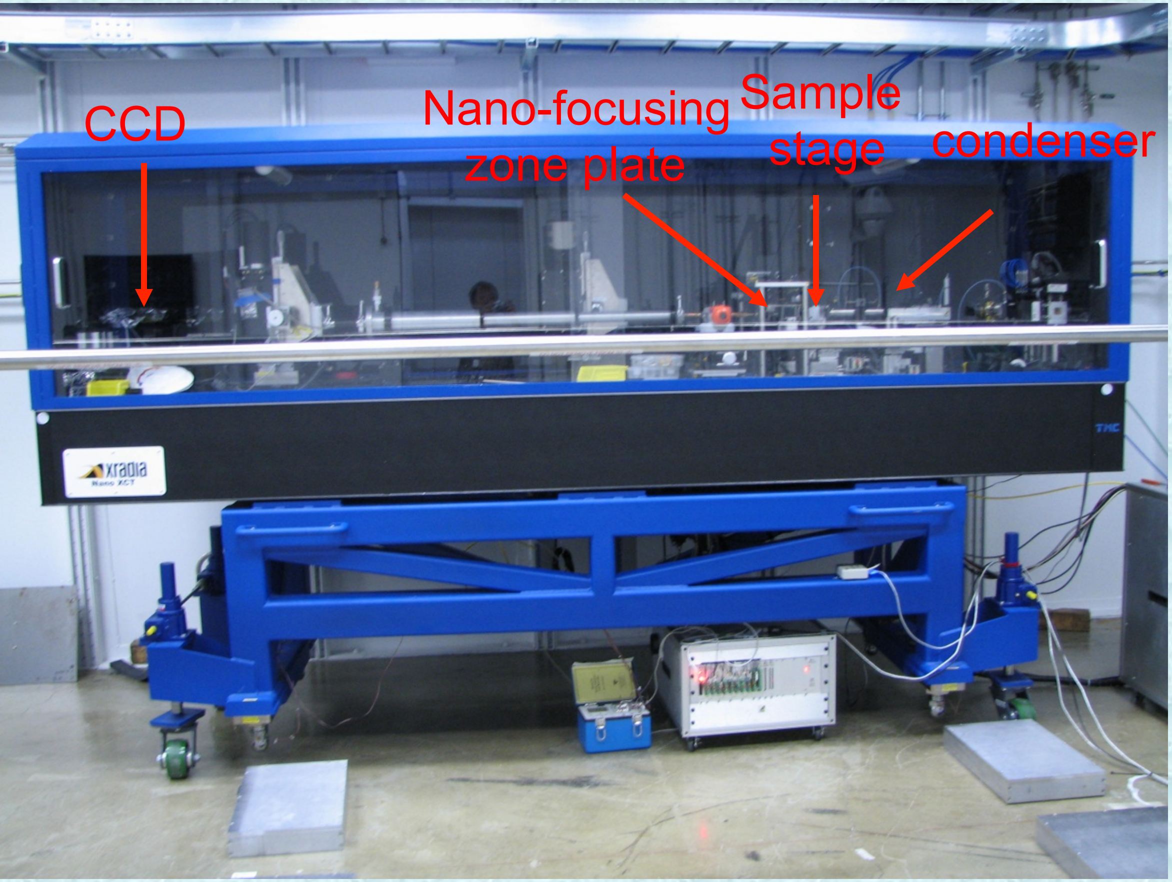

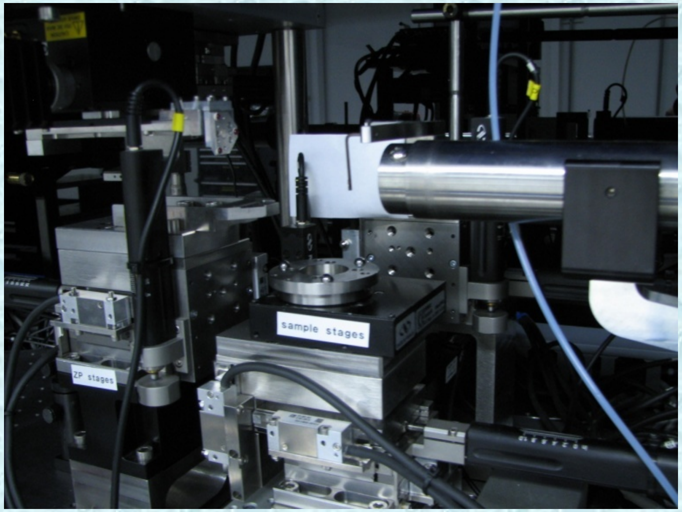

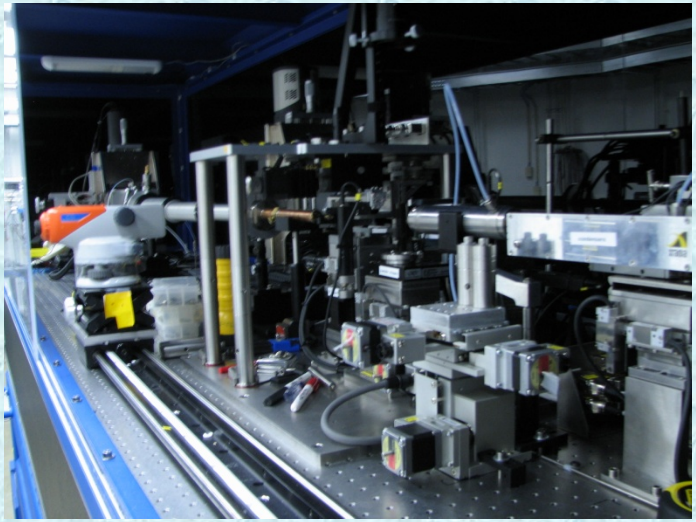

Beamline capabilities:

Full field imaging with 180 degrees data collection;

3d reconstruction with FOV 30 microns and 30 nm resolution

TXM setup vs. TEM

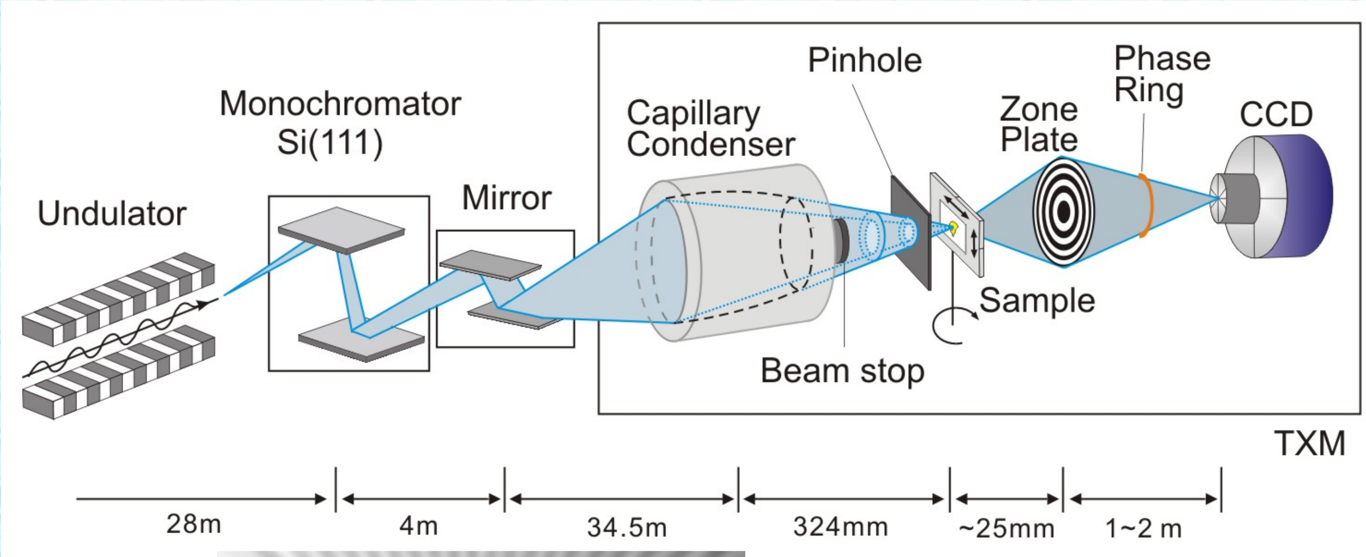

XANES-tomo

TEM

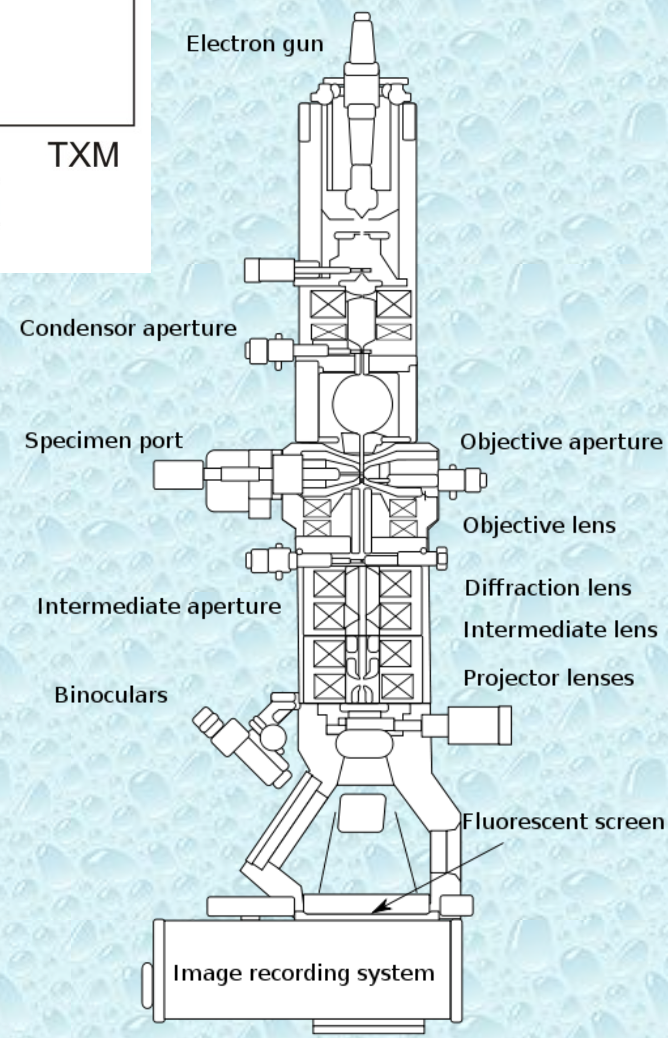

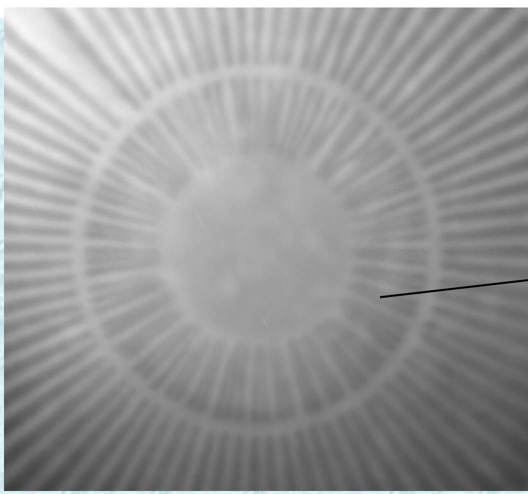

30 nm
feature

Beamline capabilities:
Full field imaging with 180 degrees data collection;
3d reconstruction with FOV 30 microns and 30 nm
require uniform illumination for FOV (diffuser
sometimes is used to create incoherent uniform beam)

HP 3d + valence

Pressure induced charge transfer in multi-ferroic system $BiNiO_3$

The phase transition can be induced by both pressure and temperature. The Structure evolution as a function of the temperature shows huge negative thermal expansion

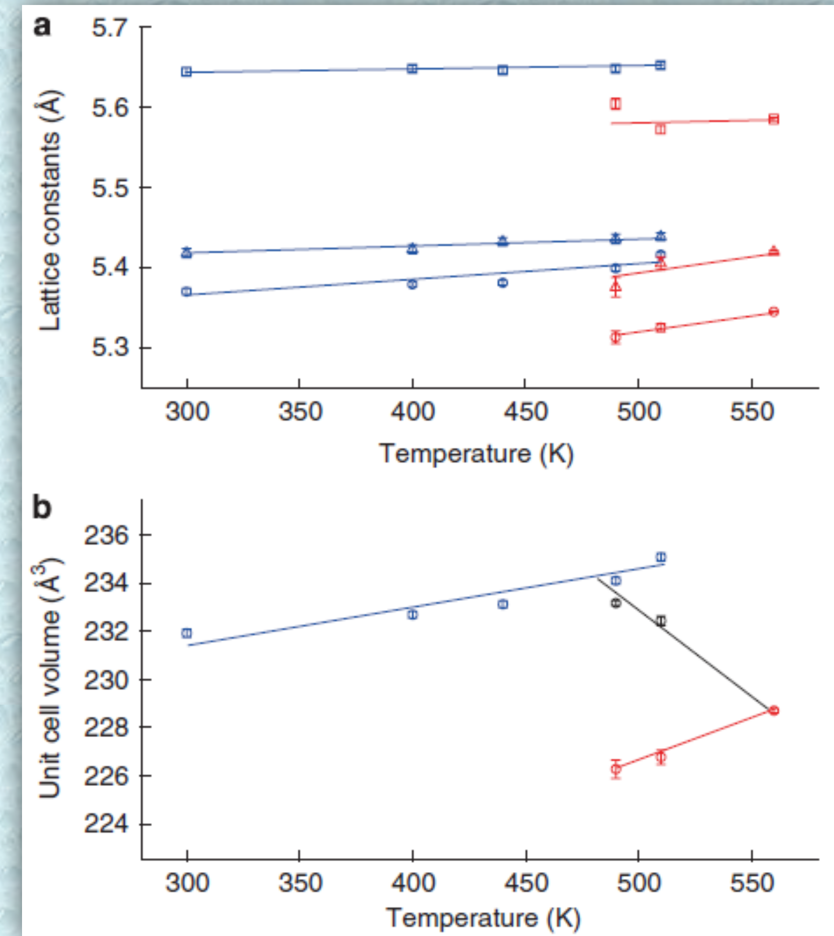

Structural evolution of $BiNiO_3$ at elevated temperatures under a constant pressure of 1.8 Gpa

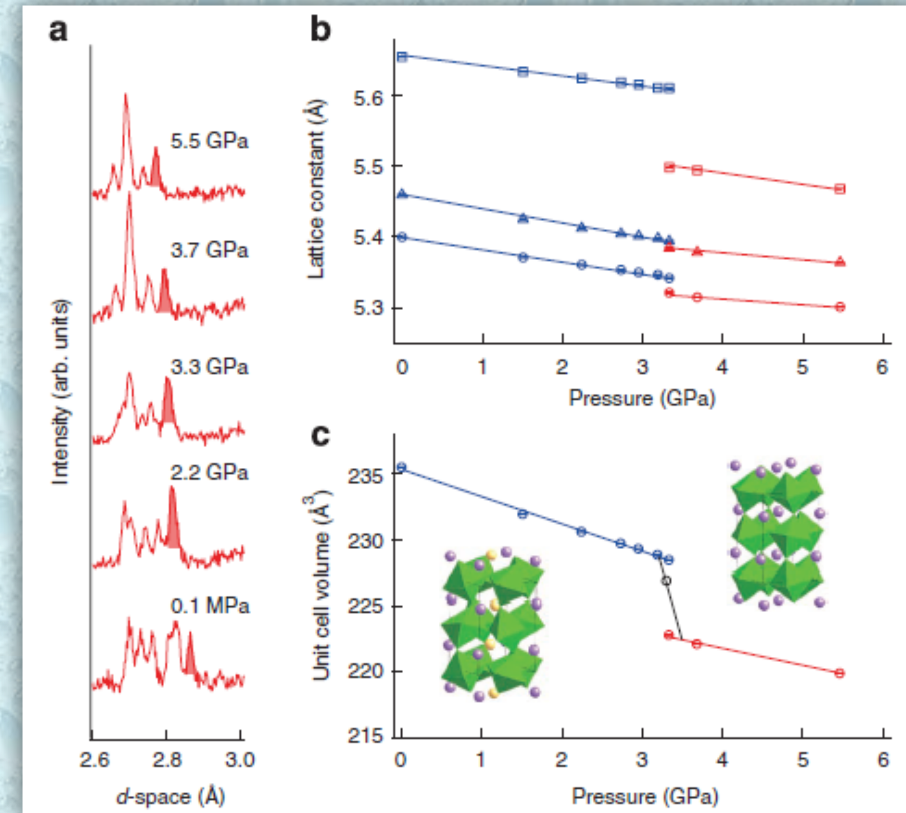

XRD data shows phase transition induced by pressure.

LPT ($Bi^{3+}_{0.5}Bi^{5+}_{0.5}Ni^{2+}O_3$) to HPT ($Bi^{3+}Ni^{3+}O_3$)

Azuma et al. Nat. Comm (2011)

三维价态分布成像

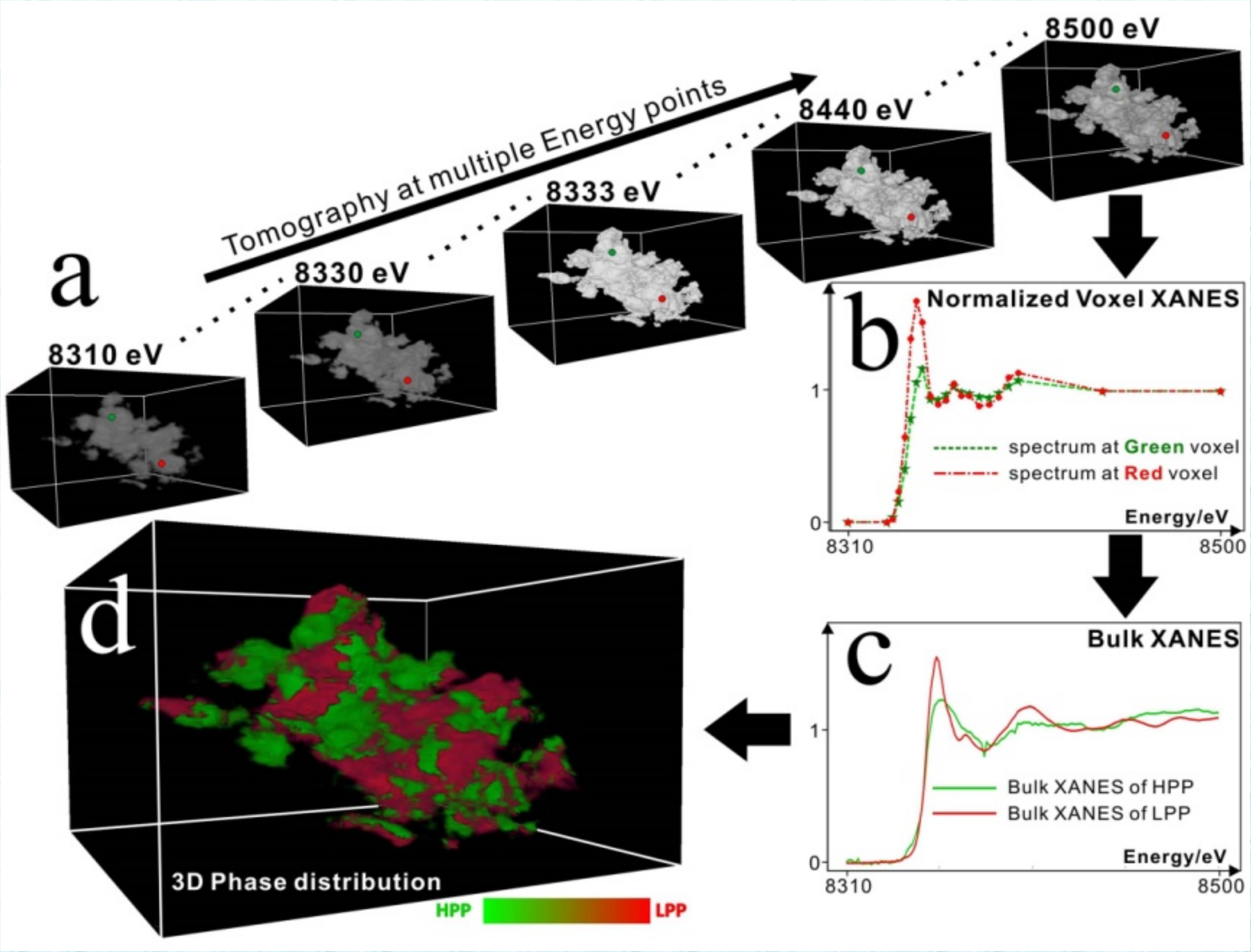

a
Tomography at multiple Energy points
8310 eV
8330 eV
8333 eV
8440 eV
8500 eV
b
Normalized Voxel XANES
spectrum at Green voxel
spectrum at Red voxel
Energy/eV
8310
8500
c
Bulk XANES
Bulk XANES of HPP
Bulk XANES of LPP
Energy/eV
8310
8500
d
3D Phase distribution
HPP
LPP

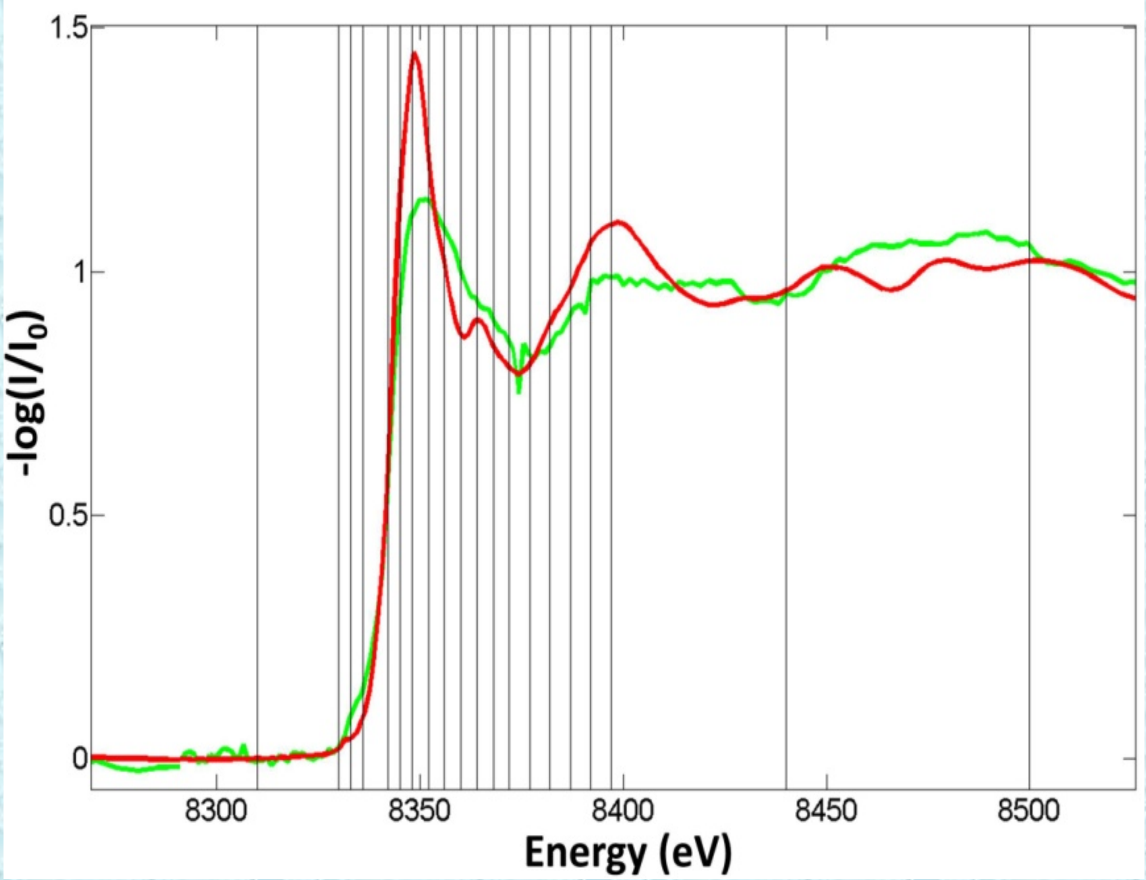

1.5
1
0.5
0
-log(I/I$_0$)
8300
8350
8400
8450
8500
Energy (eV)

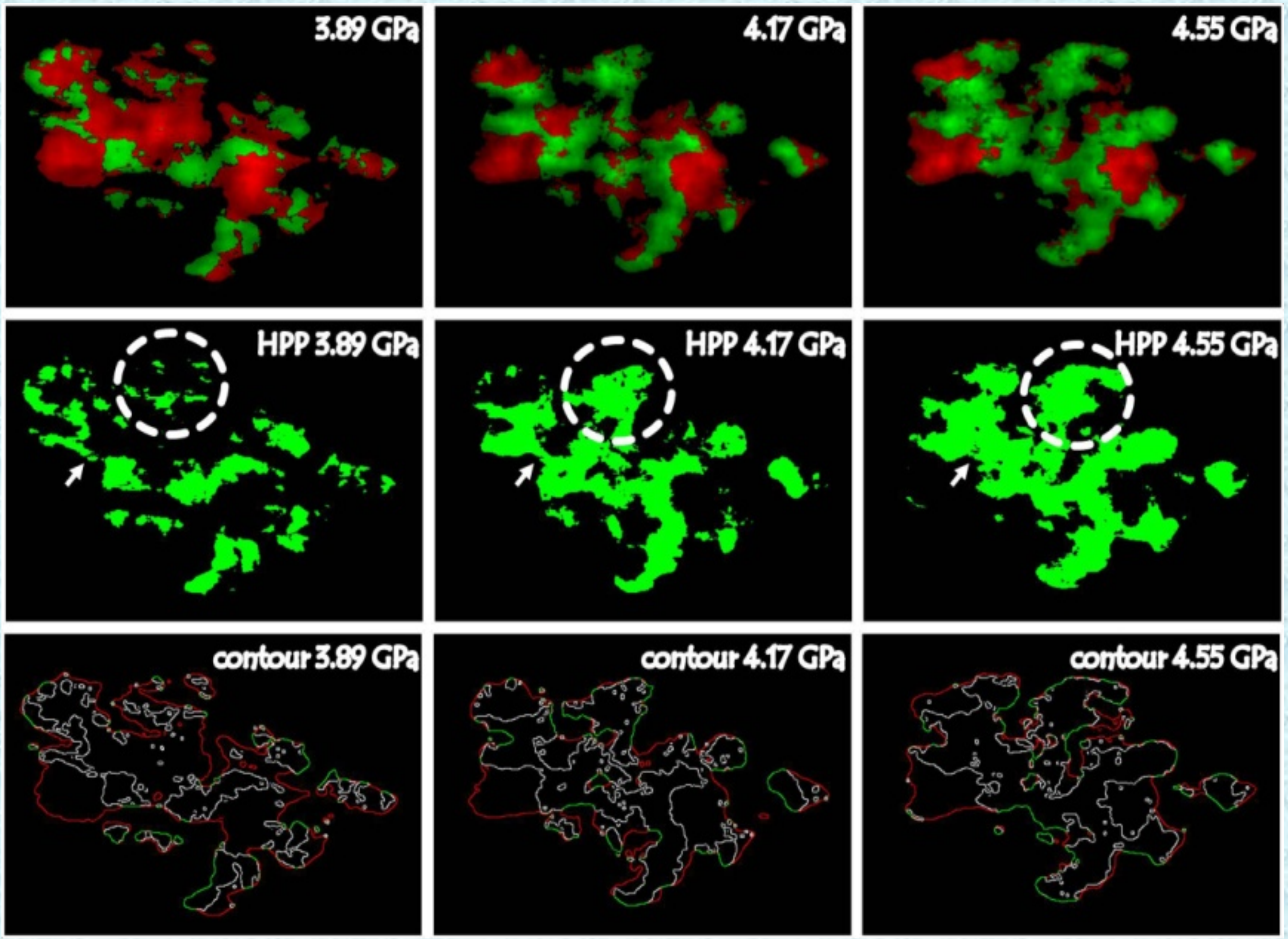
3.89 GPa
4.17 GPa
4.55 GPa
HPP 3.89 GPa
HPP 4.17 GPa
HPP 4.55 GPa
contour 3.89 GPa
contour 4.17 GPa
contour 4.55 GPa

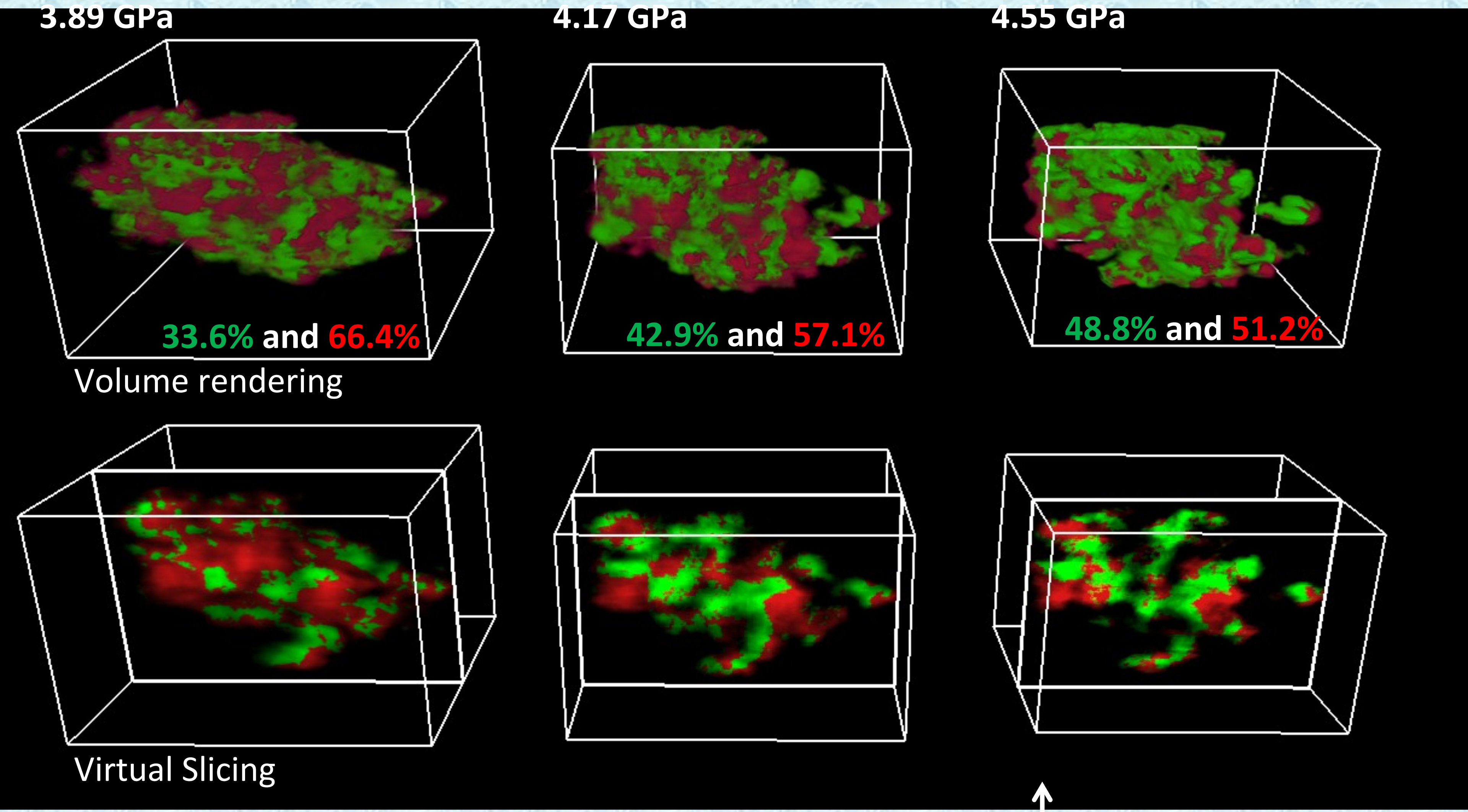

LPP in Red and **HPP in Green**. 3D XANES as a function of environment pressure.
You can see the HPP (green) growing and the LPP (red) shrinking.
The pressure induced phase transition is visualized in 3D.

Worth to mention that this is 5D analysis (x,y,z,E,P)

Liu et al. APL, 2014

TXM application to EoS of amorphous materials

a-GeO2

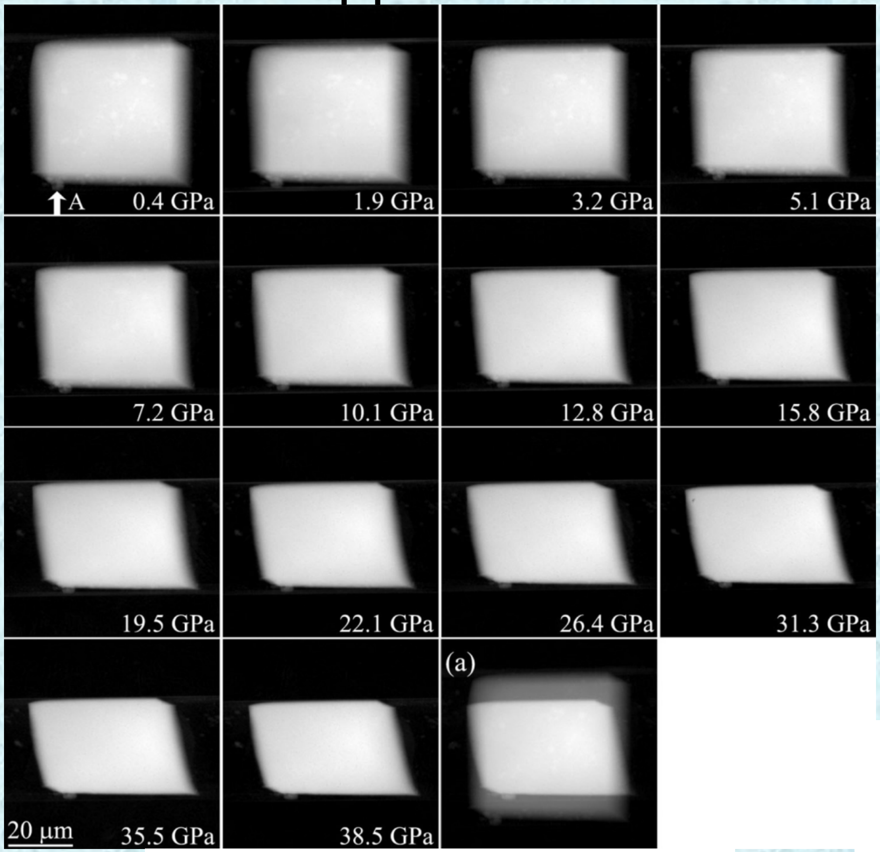

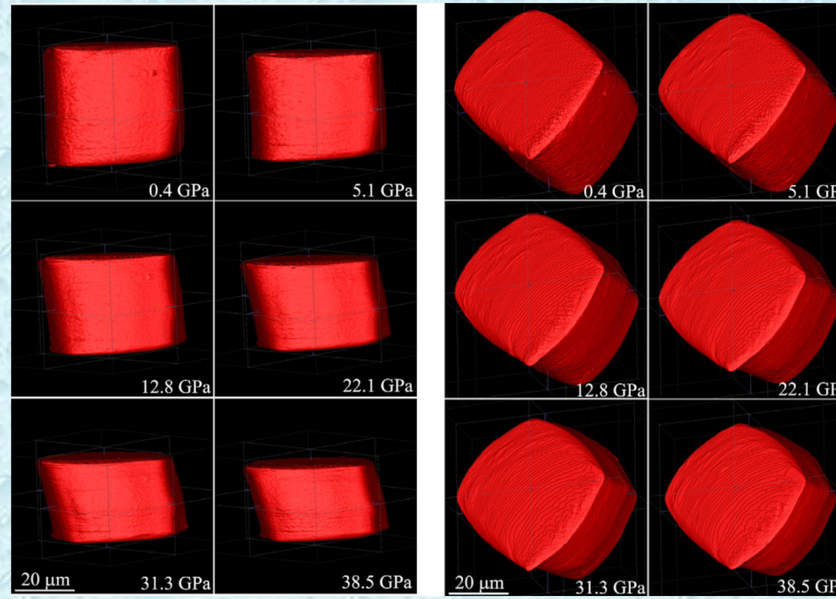

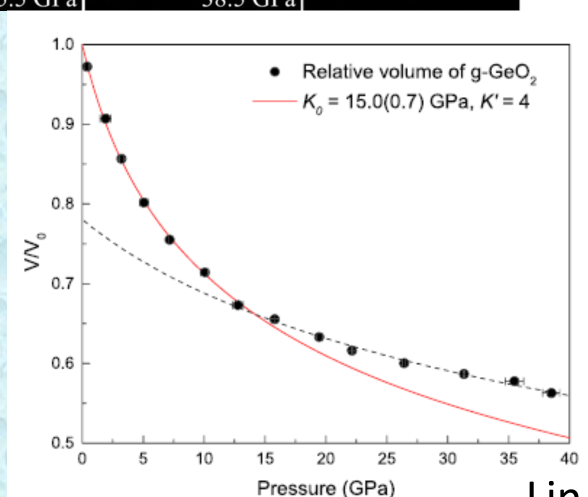

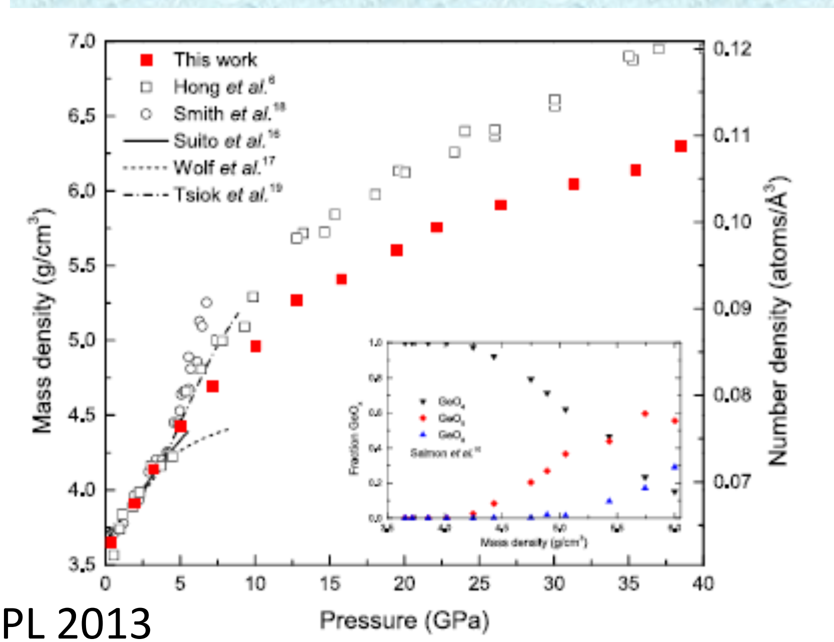

Lin et al. APL 2013

BMG

Non-cubic Power Law for Density of Metallic Glasses

TXM

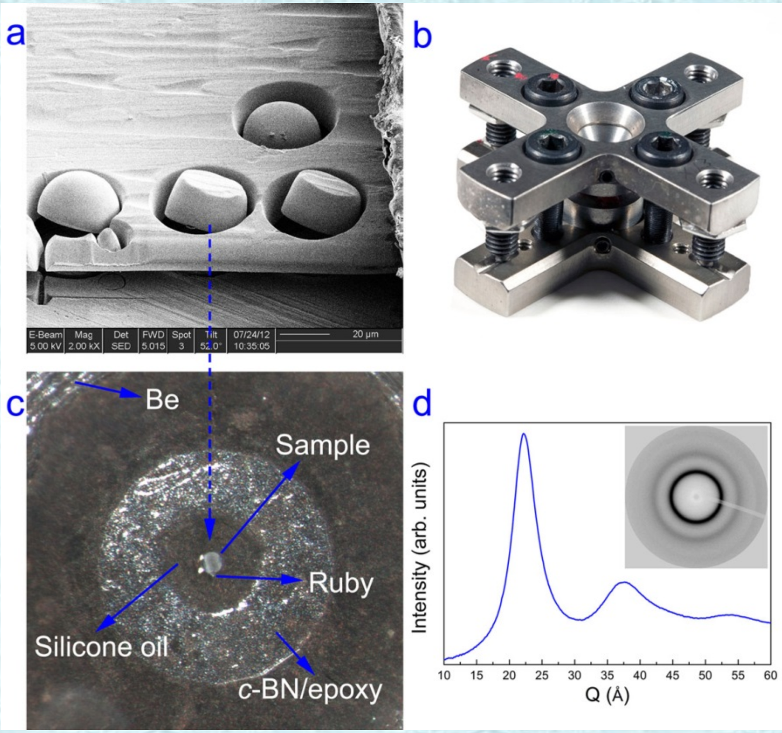

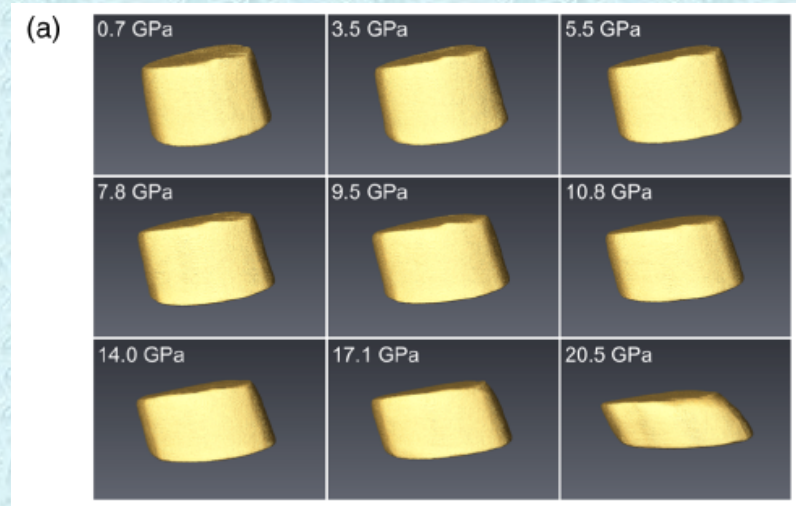

$$\rho_{P_{n+1}} = \rho_{P_n} + \int_{P_n}^{P_{n+1}} (1+\alpha\gamma T)/(V_P^2 - 4V_S^2/3)\,dP$$

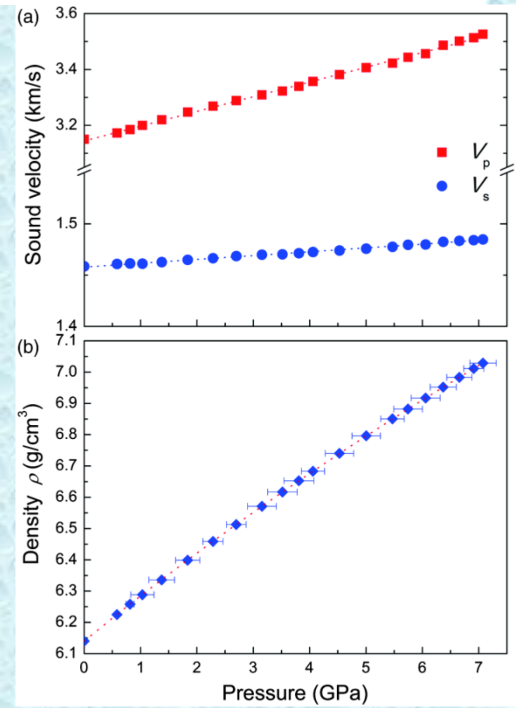

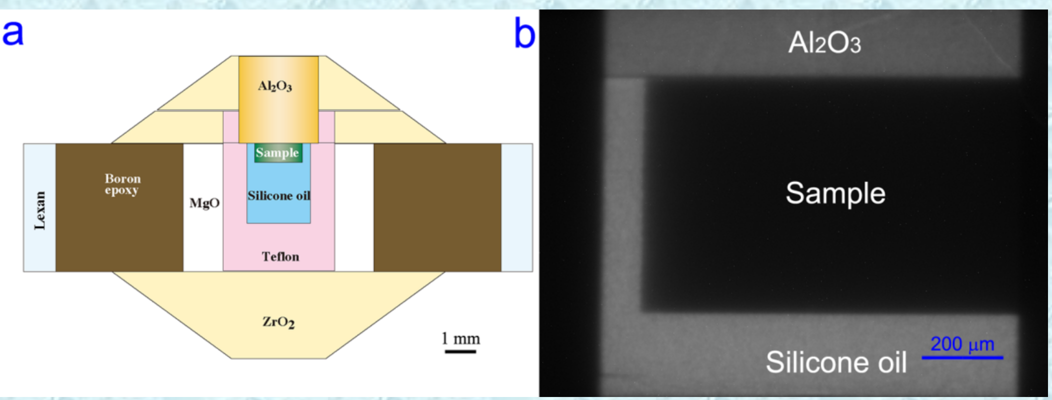

Ultrasonic

Zeng et al. PRL 2014

High pressure imaging outlook

Imaging as a direct way to watch the evolution of physical property under pressure would tremendously help researches on

- Pressure induced phase transition mechanism;
- Stress/strain, morphology, rheology and dynamics;
- Surface / interface, chemical interaction, valence distributions;
- Equation of State for liquid and amorphous materials;
- Electric and magnetic domain studies with applied external fields and pressure;

High pressure community will largely benefit from advanced imaging techniques from advanced synchrotron radiation techniques.

Acknowledgments

Financial support: EFree, HPSTAR, DOE-BES

Dave Mao, Charles Zeng, Junyue Wang @ HPSynC
Wendy Mao, Yu Lin, Yingxia Shi @ Stanford University
Steve Wang, Wenjun Liu, Ross Harder @APS,
Yijin Liu @ SSRL
Tiqiao Xiao, Guangzhao Zhou @ SSRF
Ian Robinson @ UCL
Jianwei Miao @ UCLA
Huaidong Jiang @ Shandong University